THE JOURNAL OF PHYSICAL CHEMISTRY B

pubs.acs.org/JPCB Article

Role of Cholesterol and Its Immediate Biosynthetic Precursors in Membrane Dynamics and Heterogeneity: Implications for Health and Disease

Sandeep Shrivastava,[⊥] Yamuna Devi Paila,[⊥] Mamata Kombrabail, G. Krishnamoorthy, and Amitabha Chattopadhyay*

Cite This: *J. Phys. Chem. B* 2020, 124, 6312–6320 Read Online

ACCESS | Metrics & More | Article Recommendations | Supporting Information

ABSTRACT: Cholesterol is an indispensible component of cellular membranes in higher eukaryotes and plays a vital role in many cellular functions. 7-Dehydrocholesterol (7-DHC) and desmosterol represent two immediate biosynthetic precursors of cholesterol in the Kandutsch–Russell and Bloch pathways of cholesterol biosynthesis, respectively. Although 7-DHC and desmosterol differ from cholesterol merely by a double bond, accumulation of these two immediate biosynthetic precursors due to defective cholesterol biosynthesis leads to severe developmental and neurological disorders. In this context, we explored the role of cholesterol and its immediate biosynthetic precursors (7-DHC and desmosterol) on the dynamics and heterogeneity of fluid phase POPC (1-palmitoyl-2-oleoyl-*sn*-glycero-3-phosphocholine) and gel phase DPPC (1,2-dipalmitoyl-*sn*-glycero-3-phosphocholine) membranes, using fluorescence lifetime distribution analysis of Nile Red (9-diethylamino-5*H*-benzo[α]phenoxazine-5-one) using the maximum entropy method (MEM). We show here that the membrane interfacial dynamic heterogeneity, manifested as the width of the fluorescence lifetime distribution of Nile Red, exhibited by 7-DHC and desmosterol vastly differ from that displayed by cholesterol, particularly in fluid phase membranes. We conclude that a subtle alteration in sterol structure could considerably alter dynamic membrane heterogeneity, which could have implications in pathogenicity associated with defective cholesterol biosynthesis.

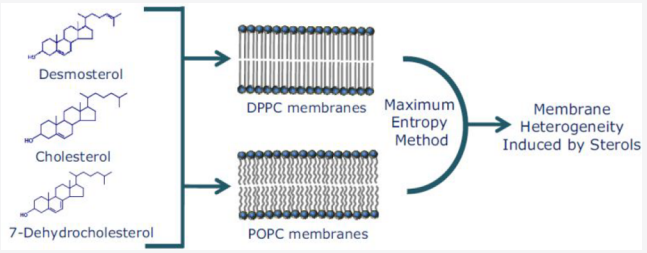

INTRODUCTION

Cholesterol is an essential component of cellular membranes in higher eukaryotes and plays a crucial role in membrane organization, dynamics, function, sorting, endocytosis of membrane proteins, early embryonic development, and entry of pathogens into host cells.[1−7] A hallmark of cholesterol organization in cellular membranes is its nonrandom distribution in a variety of ways (termed as membrane microdomains).[8−10] Domain organization is believed to be crucial for the maintenance of membrane function.

Cholesterol is the major sterol found in membranes of higher eukaryotes and is the final product of a stringently regulated, multistep enzymatic pathway.[11−13] There are two pathways for cholesterol biosynthesis, namely Bloch[11] and Kandutsch–Russell[13] pathways (see Figure 1). Interestingly, the relative contribution of these two pathways displays age, tissue, and cell-type dependence.[14−16] The unique molecular structure of cholesterol has been fine-tuned over a very long time scale of natural evolution.[17,18] In an elegant hypothesis, Bloch speculated that the cholesterol biosynthetic pathway parallels sterol evolution (termed the "Bloch hypothesis").[19] In other words, cholesterol has been evolutionarily selected over a very long time scale for its ability to optimize physical properties of cell membranes of higher eukaryotes to maintain optimal membrane function. From this perspective, cholesterol precursors could be viewed as molecules with properties that differentially affect cellular function in organisms of increasing complexity. Importantly, a variety of inherited metabolic disorders have been attributed to defects in cholesterol biosynthesis pathways (see below).[20,21] For this reason, comparative studies of the effects of cholesterol and its evolutionary biosynthetic precursors on membrane physical properties assume relevance.

In the Kandutsch–Russell pathway of cholesterol biosynthesis, 7-dehydrocholesterol (7-DHC) is the immediate biosynthetic precursor of cholesterol (Figure 1). 7-DHC is reduced to cholesterol in the final step of biosynthesis by the enzyme 3β-hydroxy-steroid-Δ^7-reductase (7-DHCR). 7-DHC varies from cholesterol only by a double bond at the seventh position of the sterol ring (see Figure 1).[13] 7-DHC gets

Received: May 14, 2020
Revised: June 25, 2020
Published: June 25, 2020

https://dx.doi.org/10.1021/acs.jpcb.0c04338
J. Phys. Chem. B 2020, 124, 6312–6320

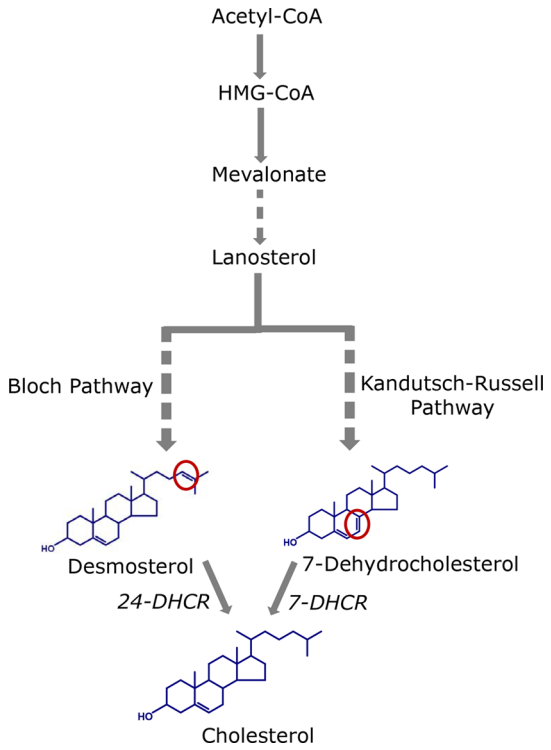

Figure 1. A schematic showing the Bloch and Kandutsch−Russell pathways for cholesterol biosynthesis. The chemical structures of the immediate biosynthetic precursors of cholesterol in both pathways are shown, along with the structure of cholesterol. 7-DHC and desmosterol are immediate biosynthetic precursors of cholesterol in the Kandutsch−Russell and Bloch pathways, respectively, and are reduced to cholesterol in the final steps of the pathways by the enzymes 7 DHCR and 24 DHCR. 7-DHC and desmosterol differ from cholesterol only in a double bond at the 7th position in the sterol ling and 24th position in the alkyl chain, respectively (highlighted in their chemical structures).

accumulated in a neurological disorder termed Smith−Lemli−Opitz syndrome (SLOS), which is a severe congenital and developmental malformation syndrome.[22,23] The molecular etiology leading to SLOS lies in mutations in the gene encoding 7-DHCR. SLOS is clinically diagnosed by elevated plasma levels of 7-DHC and reduced levels of cholesterol to 7-DHC ratio.[22−26] In the Bloch pathway, however, desmosterol is the immediate biosynthetic precursor of cholesterol, which differs from cholesterol merely in a double bond in the flexible alkyl side chain at the 24th position (Figure 1). In the final step of the Bloch pathway, desmosterol is converted to cholesterol by the enzyme 3β-hydroxy-steroid-Δ^{24}-reductase (24-DHCR). Accumulation of desmosterol results in desmosterolosis,[27] caused by mutations in the gene encoding 24-DHCR. Desmosterolosis is clinically characterized by elevated levels of desmosterol accompanied by reduced levels of cholesterol, resulting in severe developmental and neurological dysfunctions.[20,27,28]

As stated above, the chemical structure of cholesterol has been intricately fine-tuned over the course of natural evolution.[17,18] This is validated by the fact that several structural features such as an intact alicyclic chain, free 3β−OH group, planar Δ^5(6) double bond, angular methyl groups, and a branched 7-carbon alkyl chain at the 17β-position, were all found to be essential for complex biological functions carried out by cholesterol.[29−32] As a result, the function of membrane proteins (such as receptors and ion channels) that require cholesterol are not supported by even very close analogues of cholesterol differing from cholesterol in a subtle way.[25,26,28,33−36]

Biological membranes are known to display heterogeneity that could be manifested as spatial or temporal domains.[9] Spatial heterogeneity is known to give rise to microdomains in membranes, whereas temporal heterogeneity regulates dynamic properties of membranes.[9,37] Interestingly, cholesterol has been previously reported to modulate membrane heterogeneity.[37,38] In this work, we have monitored the role of cholesterol and its immediate biosynthetic precursors (7-DHC and desmosterol) in the dynamics and heterogeneity of fluid POPC (1-palmitoyl-2-oleoyl-*sn*-glycero-3-phosphocholine) and gel phase DPPC (1,2-dipalmitoyl-*sn*-glycero-3-phosphocholine) membranes. For this, we utilized fluorescence lifetime distribution analysis of the fluorescent probe Nile Red (9-diethylamino-5*H*-benzo[α]phenoxazine-5-one) using the maximum entropy method (MEM). Nile Red is a polarity-sensitive fluorescent membrane probe[39] and has been effectively used for monitoring temporal heterogeneity in model and biological membranes.[37,38] We show here that immediate biosynthetic precursors of cholesterol, 7-DHC and desmosterol, differ considerably from cholesterol in inducing membrane heterogeneity. Our results demonstrate that subtle alterations in sterol structure could alter dynamic membrane heterogeneity in a significant manner, with potential implications in pathophysiology associated with defective cholesterol biosynthesis.

EXPERIMENTAL SECTION

Materials. 1,2-Dimyristoyl-*sn*-glycero-3-phosphocholine (DMPC), cholesterol, desmosterol, and 7-DHC were purchased from Sigma Chemical Co. (St. Louis, MO). DPPC and POPC were obtained from Avanti Polar Lipids (Alabaster, AL). Nile Red was from Molecular Probes/Invitrogen (Eugene, OR). The concentration of stock solution of Nile Red was measured using its molar absorption coefficient (ε) of 45 000 M^{-1} cm^{-1} at 552 nm.[40] See the Supporting Information (section S1) for more details.

Sample Preparation. All experiments were carried out using large unilamellar vesicles (LUVs) of either DPPC or POPC with diameters of ∼100 nm containing increasing concentrations (0−50 mol %) of a given sterol (cholesterol or 7-DHC or desmosterol) and 1 mol % fluorescent probe (Nile Red). In particular, 320 nmol of total lipid (phospholipid and sterol) and 3.2 nmol of fluorescent probe were mixed well and dried under a stream of nitrogen while being warmed gently (∼35 °C). Large unilamellar vesicles (LUVs) were prepared as described previously[41] (see the Supporting Information (section S2) for more details).

Steady State Fluorescence Measurements. Steady state fluorescence measurements were performed using a quartz cuvette of 1 cm path length in a Hitachi F-4010 spectrofluorometer (Tokyo, Japan). For all measurements, Nile Red was excited at 550 nm and excitation/emission slits with 5 nm bandpass were used (see the Supporting Information (section S3) for more details).

Time-Resolved Fluorescence Measurements. Picosecond time domain fluorescence intensity decay measurements were carried out using a time-correlated single photon counting (TCSPC) setup (see the Supporting Information (section S4) for more details).

https://dx.doi.org/10.1021/acs.jpcb.0c04338
J. Phys. Chem. B 2020, 124, 6312−6320

Maximum Entropy Method (MEM) Analysis of Fluorescence Intensity Decay. Fluorescence decay data were analyzed using MEM, which offers an unbiased approach of data analysis[37,38,42−44] (see the Supporting Information (section S5) for more details).

RESULTS

Nile Red is an uncharged fluorescent probe and its fluorescence is dependent on the polarity of its immediate environment due to a large change in its dipole moment upon excitation.[45−47] In particular, it has been used for monitoring heterogeneity in membranes (manifested as the width of the fluorescence lifetime distribution of Nile Red) specifically for membranes containing cholesterol.[37,38,48] Figure 2 shows the

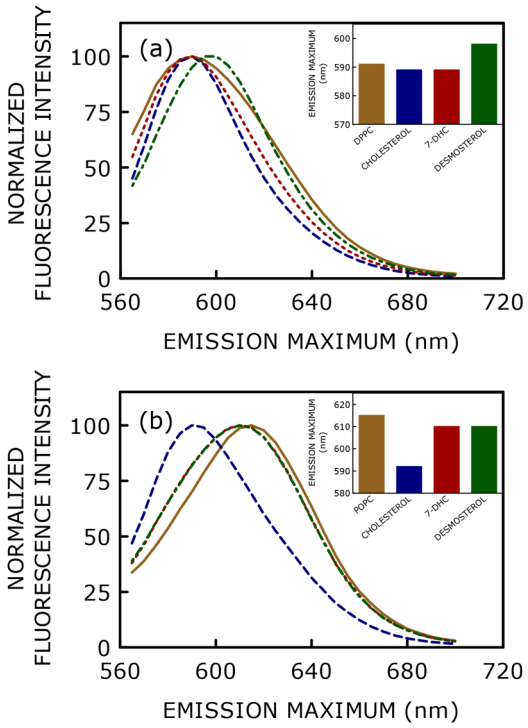

Figure 2. Fluorescence emission spectra of Nile Red in (a) DPPC and (b) POPC membranes. Representative fluorescence spectra of Nile Red in membranes in the absence of sterol (—, brown), and containing 50 mol % of cholesterol (− − − , blue), 7-DHC (---, red), or desmosterol (—·—, green) are shown. Fluorescence emission spectra are intensity-normalized at the respective emission maximum. Fluorescence measurements were carried out at room temperature (~23 °C). The excitation wavelength used was 550 nm. The ratio of Nile Red to total lipid was 1:100 (mol/mol), and the total lipid concentration was 0.21 mM in all cases. See the Experimental Section for other details.

fluorescence emission spectra of Nile Red in (a) DPPC and (b) POPC membranes in the presence of 50 mol % sterol (cholesterol or 7-DHC or desmosterol). The inset shows the corresponding emission maxima. Figure 2a shows that the emission maximum of Nile Red in gel phase DPPC membranes was 591 nm. The corresponding emission maximum for Nile Red in fluid (liquid-disordered) phase POPC membranes was 615 nm (see Figure 2b) and exhibited a considerable red shift of 24 nm. This is due to increased water penetration in the fluid phase resulting in a polar environment for the fluorophore.

The phase properties of membranes depend on the amount of sterol present in them. Above a threshold concentration of cholesterol, both DPPC and POPC exist in the liquid-ordered phase,[49,50] characterized by ordered lipid acyl chains (like gel phase) and high lateral mobility (like fluid phase). In DPPC membranes containing 50 mol % cholesterol (liquid-ordered phase), the emission maximum of Nile Red was found to be at 589 nm, thereby exhibiting a slight blue shift of 2 nm relative to DPPC alone (see Figure 2a). The emission maximum of Nile Red in DPPC containing 50 mol % 7-DHC and desmosterol was found to be at 589 and 598 nm, respectively.

As stated above, the emission maximum of Nile Red in POPC membranes was found to be at 615 nm (see Figure 2b). In POPC membranes containing 50 mol % cholesterol, the emission maximum of Nile Red displayed a large blue shift (~23 nm) and was at 592 nm (see Figure 2b). This shift in emission maximum could be due to a more compact environment (relative to fluid POPC membranes) around Nile Red in the liquid-ordered phase, resulting in less water penetration. Interestingly, the fluorescence emission maximum of Nile Red in POPC membranes with 50 mol % of either 7-DHC or desmosterol was found to be 610 nm.

Analysis of Time-Resolved Fluorescence of Nile Red in Membranes Containing Cholesterol and Its Immediate Biosynthetic Precursors. Fluorescence lifetime and the width of the fluorescence lifetime distribution of membrane incorporated Nile Red analyzed by MEM provide information about membrane properties such as polarity and dynamic (temporal) heterogeneity.[37,38] Fluorescence lifetimes of Nile Red in membranes containing cholesterol and its immediate biosynthetic precursors were analyzed first by the discrete analysis method. All fluorescence decays could be fitted well with a triexponential function. A standard decay profile with its triexponential fitting and the statistical parameters used to test the goodness of the fit is shown in Figure S1. Representative values of fluorescence lifetimes of Nile Red in DPPC and POPC membranes, calculated using eq S1 (see the Supporting Information), are shown in Tables 1 and 2. The amplitude-

Table 1. Representative Fluorescence Lifetimes of Nile Red in DPPC Membranes in the Presence of Sterols[a]

sterol content (mol %)	α_1	τ_1 (ns)	α_2	τ_2 (ns)	α_3	τ_3 (ns)
(a) Cholesterol						
0	0.19	0.55	0.39	2.88	0.42	5.46
10	0.05	0.27	0.28	3.03	0.67	6.96
30	0.03	0.70	0.23	4.75	0.74	7.36
50	0.03	0.71	0.17	6.91	0.80	7.10
(b) 7-DHC						
0	0.19	0.63	0.28	2.42	0.53	4.98
10	0.19	0.59	0.32	2.87	0.49	6.12
30	0.03	0.45	0.27	2.49	0.70	6.56
50	0.07	0.63	0.18	2.52	0.75	6.74
(c) Desmosterol						
0	0.22	0.69	0.35	3.21	0.43	5.26
10	0.11	0.58	0.21	2.04	0.68	5.63
30	0.06	1.35	0.29	2.91	0.65	5.71
50	0.11	0.93	0.23	3.17	0.66	6.25

[a]The excitation wavelength was 575 nm, and emission was monitored at 620 nm in all cases. The concentration of total lipid was 0.21 mM, and the ratio of Nile Red to total lipid was 1:100 (mol/mol). Measurements were carried out at room temperature (~23 °C). See the Experimental Section for other details.

https://dx.doi.org/10.1021/acs.jpcb.0c04338
J. Phys. Chem. B 2020, 124, 6312−6320

Table 2. Representative Fluorescence Lifetimes of Nile Red in POPC Membranes in the Presence of Sterols[b]

sterol content (mol %)	α_1	τ_1 (ns)	α_2	τ_2 (ns)	α_3	τ_3 (ns)
(a) Cholesterol						
0	0.12	0.50	0.30	2.85	0.58	4.30
10	0.09	0.64	0.11	2.57	0.80	4.27
30	0.03	0.72	0.17	2.68	0.80	5.24
50	0.06	0.55	0.10	4.10	0.84	5.85
(b) 7-DHC						
0	0.11	0.46	0.20	2.49	0.69	4.15
10	0.09	0.48	0.37	2.79	0.54	4.44
30	0.14	0.55	0.20	2.30	0.66	4.26
50	0.17	0.26	0.22	2.03	0.61	4.57
(c) Desmosterol						
0	0.10	0.51	0.35	2.95	0.55	4.34
10	0.13	0.88	0.15	2.93	0.72	4.09
30	0.10	0.48	0.35	2.86	0.55	4.47
50	0.10	0.53	0.34	2.89	0.56	4.58

[b]The excitation wavelength was 575 nm, and emission was monitored at 620 nm in all cases. The concentration of total lipid was 0.21 mM, and the ratio of Nile Red to total lipid was 1:100 (mol/mol). Measurements were carried out at room temperature (~23 °C). See the Experimental Section for other details.

averaged mean fluorescence lifetimes (τ_m) were calculated using eq S2 and are shown in Figure 3. We decided to use the mean fluorescence lifetime as a key parameter for analyzing the lifetime data of Nile Red incorporated into membranes, as it is independent of the number of exponentials used to fit the time-resolved fluorescence decay.

The amplitude-averaged mean fluorescence lifetimes of Nile Red in gel phase DPPC membranes containing various sterols are shown in Figure 3a. The mean fluorescence lifetime of Nile Red in DPPC membranes was found to be ~3.5 ns. We observed a progressive increase in mean fluorescence lifetime of Nile Red with increasing cholesterol content in the membrane. At the highest concentration of cholesterol used (50 mol %), the mean fluorescence lifetime of Nile Red was ~6.9 ns, amounting to an increase of ~97%. Figure 3a shows the change in amplitude-averaged mean fluorescence lifetime of Nile Red with increasing concentrations of 7-DHC and desmosterol. In both cases, we observe an increase in mean fluorescence lifetime with increasing sterol concentration (~5.4 ns and ~4.9 ns for 7-DHC and desmosterol, respectively). However, the extent of increase in lifetime (~54% and 40% for 7-DHC and desmosterol, respectively) is much less relative to that observed with cholesterol.

Figure 3b shows the amplitude-averaged mean fluorescence lifetime of Nile Red in fluid phase POPC membranes containing increasing concentrations of sterols. The mean fluorescence lifetime of Nile Red in fluid phase POPC membranes was estimated to be ~3.4 ns. The mean fluorescence lifetime exhibited an increase with an increase in cholesterol content in the membrane and was ~5.3 ns in the presence of 50 mol % cholesterol (~56% increase). In the case of desmosterol, the corresponding change in mean fluorescence lifetime (~3.7 ns) was relatively modest (increase of ~9%). The corresponding change in mean fluorescence lifetime with increasing concentrations of 7-DHC (~3.3 ns) was negligible, and the lifetime remained, more or less, invariant. The pattern of change in mean fluorescence lifetime of Nile Red with increasing sterol concentration, therefore,

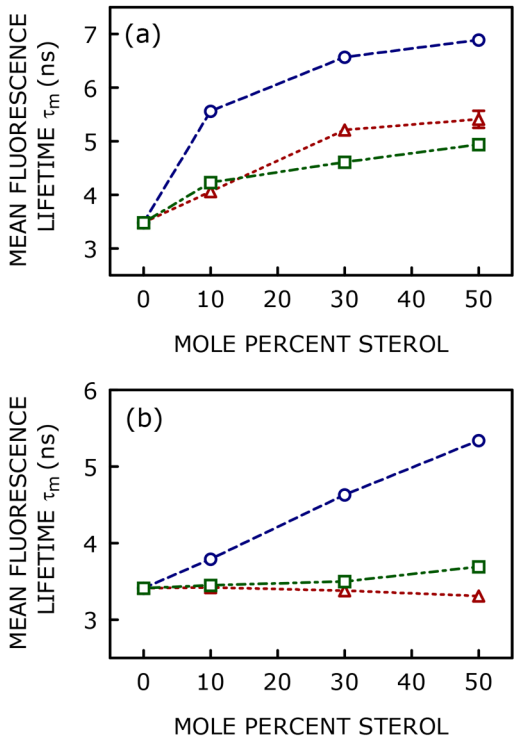

Figure 3. Amplitude-averaged mean fluorescence lifetimes of Nile Red in (a) DPPC and (b) POPC membranes as a function of increasing concentration of cholesterol (○, −−−, blue), 7-DHC (△, ---, red), and desmosterol (□, −·−, green). Mean fluorescence lifetimes were calculated from Tables 1 and 2 using eq S2. The ratio of Nile Red to total lipid was 1:100 (mol/mol), and the total lipid concentration was 0.21 mM in all cases. The excitation wavelength used was 575 nn and the emission was monitored at 620 nm. Measurements were carried out at room temperature (~23 °C). Data points shown are means ± SE of at least six independent measurements. The lines joining the data points are provided merely as viewing guides. See the Experimental Section for other details.

turned out to be very different for cholesterol and 7-DHC/desmosterol.

The increase in mean fluorescence lifetime of Nile Red with increasing cholesterol could indicate the existence of liquid-ordered-like phase, as reported previously.[38,39] Since Nile Red is an environment-sensitive probe and its fluorescence lifetime is reduced in a polar environment,[51] we interpret the increase in fluorescence lifetime of Nile Red with increasing cholesterol in fluid phase POPC membranes (Figure 3b) as being due to the reduction in water penetration in liquid-ordered phase membranes relative to fluid (liquid-disordered) phase membranes. Another factor contributing to the increase in lifetime could be slightly deeper location of Nile Red in membranes containing cholesterol.[39] However, the change in mean fluorescence lifetime in fluid phase POPC membranes in the presence of 7-DHC and desmosterol appears relatively modest or negligible. This could be due to the difference in membrane organization in the case of 7-DHC/desmosterol relative to cholesterol. It is interesting to conjecture whether such subtle yet distinct differences at the membrane level could contribute to pathogenicity associated with desmosterol and 7-DHC.

The mechanism underlying the change in mean fluorescence lifetime of Nile Red with increasing sterols in the case of gel phase DPPC membranes (Figure 3a) is more complicated.

https://dx.doi.org/10.1021/acs.jpcb.0c04338
J. Phys. Chem. B 2020, 124, 6312−6320

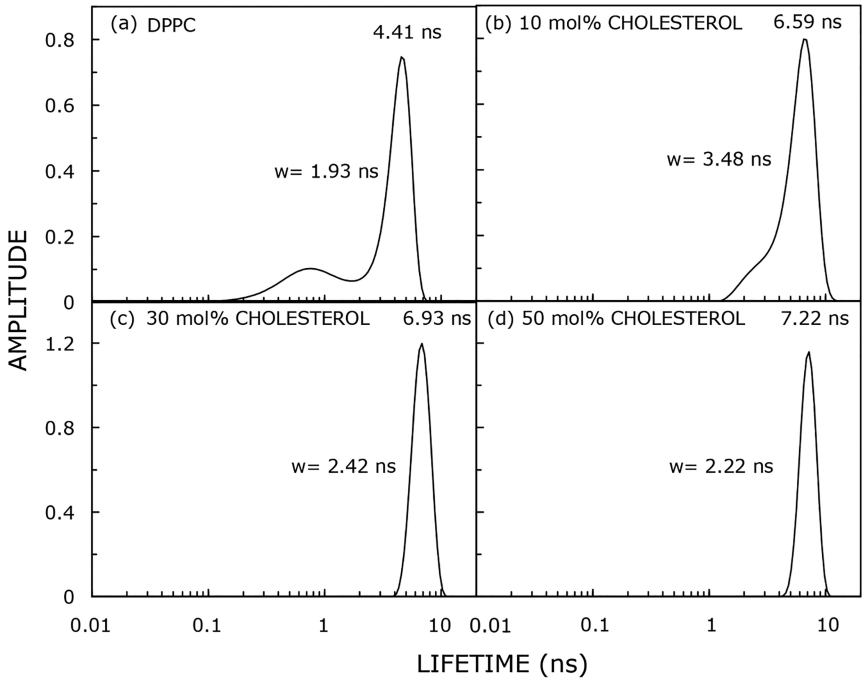

Figure 4. Representative MEM lifetime distribution of Nile Red in DPPC membranes with increasing concentrations of cholesterol. Panels a–d show the lifetime distribution of Nile Red in DPPC membranes containing (a) 0, (b) 10, (c) 30, and (d) 50 mol % cholesterol, respectively. Here *w* represents the width of the fluorescence lifetime distribution (represented as full width at half-maximum, FWHM) for the major peak whose value is indicated on the respective distribution of fluorescence lifetime. All other conditions are as in Figure 4. See the Experimental Section for other details.

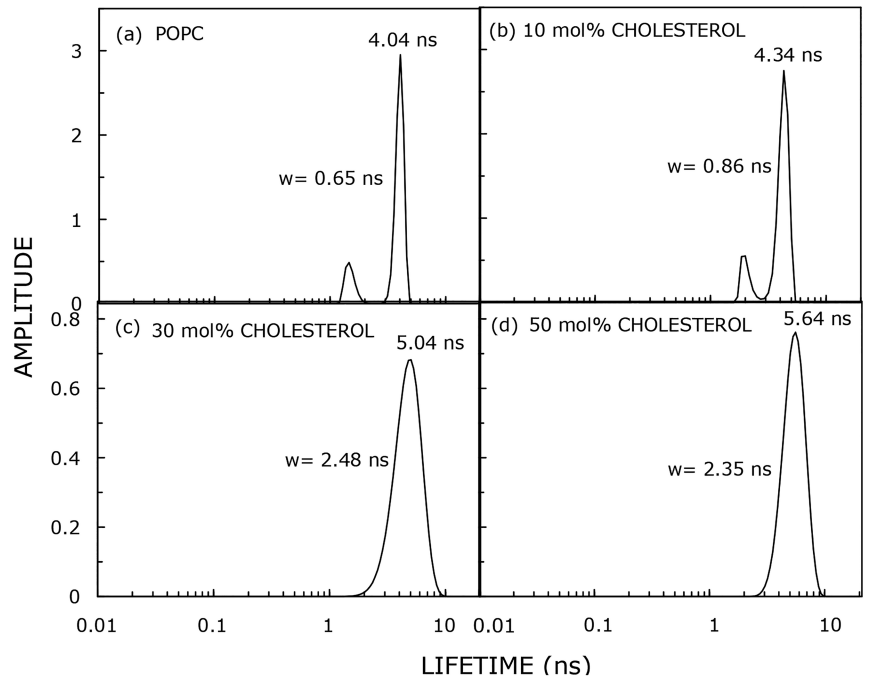

Figure 5. Representative MEM lifetime distribution of Nile Red in POPC membranes with increasing concentrations of cholesterol. Panels a–d show the lifetime distribution of Nile Red in POPC membranes containing (a) 0, (b) 10, (c) 30, and (d) 50 mol % cholesterol, respectively. Here *w* represents the width of the fluorescence lifetime distribution (represented as full width at half-maximum, FWHM) for the major peak whose position in each panel is indicated on the respective distributions of fluorescence lifetime with a number. All other conditions are as in Figure 4. See the Experimental Section for other details.

This is due to the complex and heterogeneous nature of the gel phase membrane. Previous reports on the diffusion of fluorescent lipid probes monitored using FRAP have suggested the presence of two populations of diffusing probes.[52−58] The relatively slow component is believed to represent probe diffusion in the bulk of the gel phase membrane whereas the

https://dx.doi.org/10.1021/acs.jpcb.0c04338
J. Phys. Chem. B 2020, 124, 6312−6320

faster component could be due to probe diffusion in submicroscopic linear defects formed at the interstices of relatively homogeneous gel phase regions of the membrane. Such defects are thought to be an intrinsic feature of gel phase membranes. The complication in interpreting the change in mean fluorescence lifetime of Nile Red with increasing sterols in the case of gel phase DPPC membranes arises due to the heterogeneous distribution of Nile Red in these two populations.

Lifetime Distribution of Nile Red in Membranes Containing Sterols. For fluorophores in complex systems, fluorescence decay kinetics generally exhibits considerable heterogeneity. Fluorescence lifetime distribution in such cases represents a powerful method for characterizing complex microheterogeneous assemblies such as membranes. The width of the lifetime distribution estimated using MEM provides information on the integrity and heterogeneity of complex assemblies.[37,38,48] The advantage of the MEM approach is that it is robust and model-free.[42−44] The fluorescence lifetime distributions of Nile Red in DPPC and POPC membranes containing different concentrations of cholesterol, obtained by MEM analysis are shown in Figures 4 and 5 (for details of MEM analysis, see section S5 of the Supporting Information). The representative peak positions and widths of the fluorescence lifetime distribution (full width at half-maximum (FWHM), denoted as w in Figures 4 and 5) of Nile Red in DPPC (Figure 4) and POPC (Figure 5) membranes with increasing concentrations of cholesterol are shown. It should be noted while comparing FWHM between different panels in Figures 4 and 5 that the *X*-axis (lifetime) is in log scale and not to the same scale in all panels since the peak positions are different.

The peak value of fluorescence lifetime of Nile Red could be representative of the effective polarity of a specific location in the membrane where the fluorophore resides.[51] The peak positions of the lifetime distribution of Nile Red in membranes containing cholesterol and its immediate biosynthetic precursors are shown in Figure 6. Figure 6a shows that the peak position of the lifetime distribution of Nile Red in DPPC membranes increases with increasing sterol concentration. The increase in the peak value of Nile Red at the highest cholesterol concentration (50 mol %) was ∼60%, while the corresponding increase in membranes containing highest concentration of 7-DHC and desmosterol was ∼43% and ∼29%, respectively (similar trend as in Figure 3a). Figure 6b displays the peak position of the fluorescence lifetime distribution of Nile Red in POPC membranes with increasing concentrations of sterols. The figure shows that there is a considerable increase (∼43%) in the peak value of Nile Red at the highest cholesterol concentration used (50 mol %). In contrast, the corresponding increase in 7-DHC (∼9%) and desmosterol (∼2%) was modest. The pattern of change here is similar to what was observed in Figure 3b. The salient feature is that the increase in the peak position of the fluorescence lifetime distribution of Nile Red for 7-DHC and desmosterol is much less (∼9 and 2%) compared to the corresponding change with cholesterol (∼43%).

Figure 7 shows FWHM of the lifetime distribution of Nile Red in membranes containing cholesterol and its immediate biosynthetic precursors in DPPC (Figure 7a) and POPC (Figure 7b) membranes. Interestingly, with 10 mol % cholesterol in DPPC membranes, the FWHM increases considerably (∼86%), probably indicating increased membrane heterogeneity due to the appearance of a coexisting gel/liquid-ordered phase (with more contribution from gel phase), as apparent from the phase diagram of DPPC−cholesterol.[59,60] With a further increase in cholesterol concentration, the FWHM exhibited a reduction, indicating the presence of a coexisting gel/liquid-ordered phase (with more contribution from liquid-ordered phase). In the case of 7-DHC and desmosterol, the initial increase in the FWHM was less than it was for cholesterol (∼54% and 42%, respectively). In contrast to cholesterol results, the FWHM did not exhibit any reduction in membranes containing either desmosterol or 7-DHC above 10 mol % sterol concentration. Figure 7b shows the FWHM of Nile Red in POPC membranes with increasing sterol concentration. The figure shows that there is an enormous increase (∼259%) in FWHM at 30 mol % cholesterol, followed by a plateau. In the case of 7-DHC and desmosterol, the increase in FWHM with sterol concentration continued above 30 mol % concentration (as opposed to results with cholesterol).

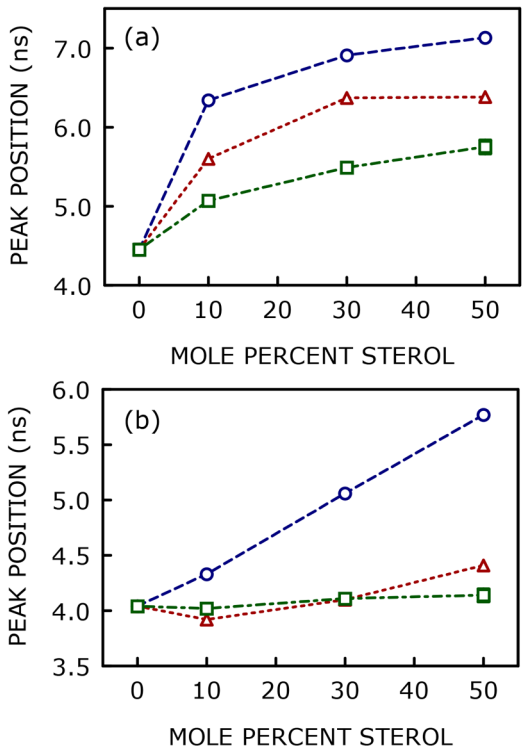

Figure 6. Peak value of fluorescence lifetime (calculated from MEM distribution of the Nile Red lifetime) in (a) DPPC and (b) POPC membranes as a function of increasing concentration of cholesterol (○, −−−), 7-DHC (△, ---), and desmosterol (□, −·−). All other conditions are as in Figure 3. The color coding is the same as in Figure 3. Data points shown are means ± SE of at least six independent measurements. The lines joining the data points are provided merely as viewing guides. See the Experimental Section for other details.

DISCUSSION

The overall objective of this work is to study the effect of cholesterol and its immediate biosynthetic precursors (7-DHC and desmosterol) on the organization and dynamics of gel and fluid phase membranes, with the long-term goal of addressing pathogenicity associated with accumulation of these immediate biosynthetic precursors due to defective cholesterol biosyn-

https://dx.doi.org/10.1021/acs.jpcb.0c04338
J. Phys. Chem. B 2020, 124, 6312−6320

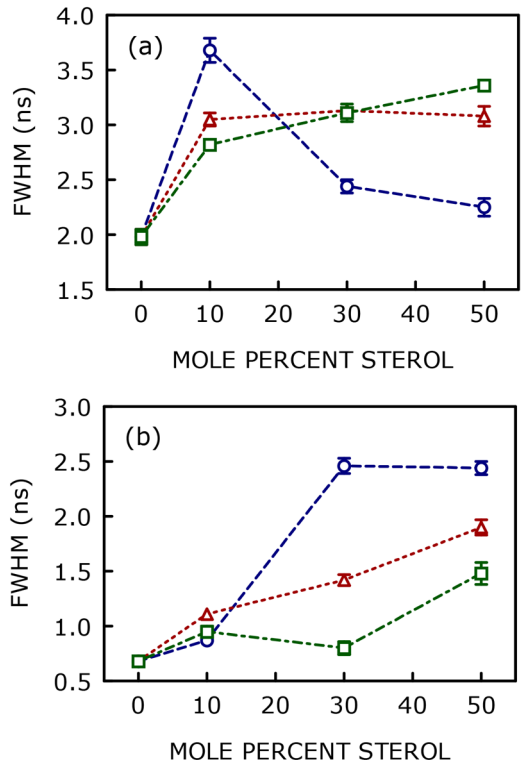

Figure 7. FWHM of Nile Red in (a) DPPC and (b) POPC membranes as a function of increasing concentration of cholesterol (○, ———), 7-DHC (△, ---), and desmosterol (□, —·—). The color coding is the same as in Figure 3. FWHM values were calculated from MEM distribution of the Nile Red lifetime. All other conditions are as in Figure 3. Data points shown are means ± SE of at least six independent measurements. The lines joining the data points are provided merely as viewing guides. See the Experimental Section for other details.

thesis. For this, we explored temporal (dynamic) heterogeneity exhibited by these closely related sterols in gel (ordered) and fluid (liquid-disordered) membranes utilizing the polarity-sensitive fluorescent membrane probe, Nile Red. Dynamic membrane heterogeneity has been previously shown to be a sensitive indicator of the immediate environment in which the fluorescent membrane probe is localized.[37,38,48,61−64] We have previously shown, using the parallax method,[65] that Nile Red is localized at the interfacial region in membranes,[39] a region characterized with unique dielectric properties and dynamics that facilitates a number of important membrane functions.[66,67] The dynamic heterogeneity obtained from analysis of the FWHM of Nile Red therefore corresponds to the membrane interface. Our present results show that membrane interfacial dynamic heterogeneity exhibited by 7-DHC and desmosterol vastly differ from that displayed by cholesterol, particularly in fluid phase membranes. This is in spite of the fact that 7-DHC and desmosterol are structurally very similar to cholesterol, differing merely by a double bond. Heterogeneity appears less in membranes containing 7-DHC or desmosterol relative to membranes containing cholesterol. In addition, water permeability appears to be higher in the case of membranes containing 7-DHC and desmosterol.

In a previous paper, we monitored the ability of various sterols in the cholesterol biosynthetic pathway to modulate membrane dipole potential.[68] The membrane dipole potential represents an important electrical property of membranes and has its origin in the electrostatic potential difference within the membrane due to the nonrandom arrangement of dipoles of polar groups in lipids and water molecules at the membrane interface.[69−72] Membrane dipole potential, whose magnitude could vary between 200 and 1000 mV, could act as a crucial determinant in the function of membrane receptors such as GPCRs.[70,71] Although cholesterol has previously been shown to increase membrane dipole potential,[73] our results showed that 7-DHC and desmosterol differ profoundly in their ability to increase membrane dipole potential (relative to cholesterol).[68] From a more biochemical perspective, the cholesterol-dependent function of membrane proteins[74] has been shown to be affected when cholesterol is replaced with 7-DHC or desmosterol. For example, we have previously shown that 7-DHC and desmosterol cannot support the function of the serotonin$_{1A}$ receptor,[25,26,28] an important G-protein coupled neurotransmitter receptor that requires membrane cholesterol for its function.[74,75]

On a broader perspective, our results demonstrate that a small change in sterol structure could considerably alter dynamic membrane heterogeneity with implications in pathogenicity associated with defective cholesterol biosynthesis. To the best of our knowledge, these results constitute one of the first reports on the difference in dynamic (temporal) membrane heterogeneity displayed by cholesterol and its immediate biosynthetic precursors (7-DHC/desmosterol). We have previously shown that the 7-DHC and desmosterol differ considerably with cholesterol with respect to their ability to increase membrane dipole potential.[68] These previous results, along with our present results, could represent the physicochemical basis of altered membrane organization in the presence of 7-DHC/desmosterol, which could provide novel insight into the mechanism of pathogenicity induced by accumulation of these precursors. We envision that a comprehensive understanding of a structure−function relationship of close biosynthetic precursors of cholesterol could lead to a better understanding of the molecular basis of diseases caused by altered sterol biosynthesis.

■ ASSOCIATED CONTENT

Supporting Information

The Supporting Information is available free of charge at https://pubs.acs.org/doi/10.1021/acs.jpcb.0c04338.

Section S1, materials; section S2, sample preparation; section S3, steady state fluorescence measurements; section S4, time-resolved fluorescence measurements; section S5, maximum entropy method (MEM) analysis of fluorescence intensity decay; representative time-resolved fluorescence intensity decay profile of Nile Red in POPC membranes (PDF)

■ AUTHOR INFORMATION

Corresponding Author

Amitabha Chattopadhyay − *CSIR-Centre for Cellular and Molecular Biology, Hyderabad 500 007, India;* orcid.org/0000-0002-2618-2565; Phone: +91-40-2719-2578; Email: amit@ccmb.res.in

Authors

Sandeep Shrivastava − *CSIR-Centre for Cellular and Molecular Biology, Hyderabad 500 007, India*

https://dx.doi.org/10.1021/acs.jpcb.0c04338
J. Phys. Chem. B 2020, 124, 6312−6320

Yamuna Devi Paila − *CSIR-Centre for Cellular and Molecular Biology, Hyderabad 500 007, India*
Mamata Kombrabail − *Department of Chemical Sciences, Tata Institute of Fundamental Research, Mumbai 400 005, India*
G. Krishnamoorthy − *Department of Chemical Sciences, Tata Institute of Fundamental Research, Mumbai 400 005, India*

Complete contact information is available at: https://pubs.acs.org/10.1021/acs.jpcb.0c04338

Author Contributions

[⊥]S.S. and Y.D.P. contributed equally to the work

Notes

The authors declare no competing financial interest.

■ ACKNOWLEDGMENTS

This work was supported by SERB Distinguished Fellowship grant (Department of Science and Technology, Govt. of India) to A.C., core support from CSIR-Centre for Cellular and Molecular Biology (A.C.) and Tata Institute of Fundamental Research (G.K.). We thank Saswata Sankar Sarkar, Suman Paul, Anjali Jha, and Sourav Haldar for helpful discussions and members of the Chattopadhyay laboratory for critically reading the manuscript and providing helpful comments.

■ REFERENCES

(1) Mouritsen, O. G.; Zuckermann, M. J. What's so special about cholesterol? *Lipids* **2004**, *39*, 1101−1113.
(2) Grouleff, J.; Irudayam, S. J.; Skeby, K. K.; Schiøtt, B. The influence of cholesterol on membrane protein structure, function, and dynamics studied by molecular dynamics simulations. *Biochim. Biophys. Acta, Biomembr.* **2015**, *1848*, 1783−1795.
(3) Simons, K.; Ikonen, E. How cells handle cholesterol. *Science* **2000**, *290*, 1721−1726.
(4) Liscum, L.; Underwood, K. W. Intracellular cholesterol transport and compartmentation. *J. Biol. Chem.* **1995**, *270*, 15443−15446.
(5) Kumar, G. A.; Chattopadhyay, A. Statin-induced chronic cholesterol depletion switches GPCR endocytosis and trafficking: insights from the serotonin$_{1A}$ receptor. *ACS Chem. Neurosci.* **2020**, *11*, 453−465.
(6) Porter, J. A.; Young, K. E.; Beachy, P. A. Cholesterol modification of hedgehog signaling proteins in animal development. *Science* **1996**, *274*, 255−259.
(7) Kumar, G. A.; Jafurulla, M.; Chattopadhyay, A. The membrane as the gatekeeper of infection: cholesterol in host-pathogen interaction. *Chem. Phys. Lipids* **2016**, *199*, 179−185.
(8) Xu, X.; London, E. The effect of sterol structure on membrane lipid domains reveals how cholesterol can induce lipid domain formation. *Biochemistry* **2000**, *39*, 843−849.
(9) Mukherjee, S.; Maxfield, F. R. Membrane domains. *Annu. Rev. Cell Dev. Biol.* **2004**, *20*, 839−866.
(10) Chaudhuri, A.; Chattopadhyay, A. Transbilayer organization of membrane cholesterol at low concentrations: implications in health and disease. *Biochim. Biophys. Acta, Biomembr.* **2011**, *1808*, 19−25.
(11) Bloch, K. The biological synthesis of cholesterol. *Science* **1965**, *150*, 19−28.
(12) Nes, W. D. Biosynthesis of cholesterol and other sterols. *Chem. Rev.* **2011**, *111*, 6423−6451.
(13) Kandutsch, A. A.; Russell, A. E. Preputial gland tumor sterols. III. A metabolic pathway from lanosterol to cholesterol. *J. Biol. Chem.* **1960**, *235*, 2256−2261.
(14) Zhang, Y.; Appelkvist, E.-L.; Kristensson, K.; Dallner, G. The lipid compositions of different regions of rat brain during development and aging. *Neurobiol. Aging* **1996**, *17*, 869−875.
(15) Thelen, K. M.; Falkai, P.; Bayer, T. A.; Lütjohann, D. Cholesterol synthesis rate in human hippocampus declines with aging. *Neurosci. Lett.* **2006**, *403*, 15−19.
(16) Mitsche, M. A.; McDonald, J. G.; Hobbs, H. H.; Cohen, J. C. Flux analysis of cholesterol biosynthesis in vivo reveals multiple tissue and cell-type specific pathways. *eLife* **2015**, *4*, No. e07999.
(17) Brown, A. J.; Galea, A. M. Cholesterol as an evolutionary response to living with oxygen. *Evolution* **2010**, *64*, 2179−2183.
(18) Kumar, G. A.; Chattopadhyay, A. Cholesterol: an evergreen molecule in biology. *Biomed. Spectrosc. Imaging* **2016**, *5*, S55−S66.
(19) Bloch, K. E. Sterol structure and membrane function. *CRC Crit. Rev. Biochem.* **1983**, *14*, 47−92.
(20) Waterham, H. R. Defects of cholesterol biosynthesis. *FEBS Lett.* **2006**, *580*, 5442−5449.
(21) Porter, F. D.; Herman, G. E. Malformation syndromes caused by disorders of cholesterol synthesis. *J. Lipid Res.* **2011**, *52*, 6−34.
(22) Waterham, H. R.; Wanders, R. J. A. Biochemical and genetic aspects of 7-dehydrocholesterol reductase and Smith-Lemli-Opitz syndrome. *Biochim. Biophys. Acta, Mol. Cell Biol. Lipids* **2000**, *1529*, 340−356.
(23) Porter, F. D. Smith-Lemli-Opitz syndrome: pathogenesis, diagnosis and management. *Eur. J. Hum. Genet.* **2008**, *16*, 535−541.
(24) Chattopadhyay, A.; Paila, Y. D. Lipid-protein interactions, regulation and dysfunction of brain cholesterol. *Biochem. Biophys. Res. Commun.* **2007**, *354*, 627−633.
(25) Singh, P.; Paila, Y. D.; Chattopadhyay, A. Differential effects of cholesterol and 7-dehydrocholesterol on the ligand binding activity of the hippocampal serotonin$_{1A}$ receptor: implications in SLOS. *Biochem. Biophys. Res. Commun.* **2007**, *358*, 495−499.
(26) Paila, Y. D.; Murty, M. R. V. S.; Vairamani, M.; Chattopadhyay, A. Signaling by the human serotonin$_{1A}$ receptor is impaired in cellular model of Smith-Lemli-Opitz syndrome. *Biochim. Biophys. Acta, Biomembr.* **2008**, *1778*, 1508−1516.
(27) FitzPatrick, D. R.; Keeling, J. W.; Evans, M. J.; Kan, A. E.; Bell, J. E.; Porteous, M. E. M.; Mills, K.; Winter, R. M.; Clayton, P. T. Clinical phenotype of desmosterolosis. *Am. J. Med. Genet.* **1998**, *75*, 145−152.
(28) Singh, P.; Saxena, R.; Paila, Y. D.; Jafurulla, M.; Chattopadhyay, A. Differential effects of cholesterol and desmosterol on the ligand binding function of the hippocampal serotonin$_{1A}$ receptor: implications in desmosterolosis. *Biochim. Biophys. Acta, Biomembr.* **2009**, *1788*, 2169−2173.
(29) Ranadive, G. N.; Lala, A. K. Sterol-phospholipid interaction in model membranes: role of C_5-C_6 double bond in cholesterol. *Biochemistry* **1987**, *26*, 2426−2431.
(30) Kumari, S. N.; Ranadive, G. N.; Lala, A. K. Growth of a yeast mutant on ring A modified cholesterol derivatives. *Biochim. Biophys. Acta, Biomembr.* **1982**, *692*, 441−446.
(31) Róg, T.; Pasenkiewicz-Gierula, M.; Vattulainen, I.; Karttunen, M. What happens if cholesterol is made smoother: importance of methyl substituents in cholesterol ring structure on phosphatidylcholine-sterol interaction. *Biophys. J.* **2007**, *92*, 3346−3357.
(32) Pöyry, S.; Róg, T.; Karttunen, M.; Vattulainen, I. Significance of cholesterol methyl groups. *J. Phys. Chem. B* **2008**, *112*, 2922−2929.
(33) Ollila, O. H. S.; Róg, T.; Karttunen, M.; Vattulainen, I. Role of sterol type on lateral pressure profiles of lipid membranes affecting membrane protein functionality: Comparison between cholesterol, desmosterol, 7-dehydrocholesterol and ketosterol. *J. Struct. Biol.* **2007**, *159*, 311−323.
(34) Vainio, S.; Jansen, M.; Koivusalo, M.; Róg, T.; Karttunen, M.; Vattulainen, I.; Ikonen, E. Significance of sterol structural specificity. Desmosterol cannot replace cholesterol in lipid rafts. *J. Biol. Chem.* **2006**, *281*, 348−355.
(35) Romanenko, V. G.; Rothblat, G. H.; Levitan, I. Modulation of endothelial inward-rectifier K^+ current by optical isomers of cholesterol. *Biophys. J.* **2002**, *83*, 3211−3222.
(36) Jafurulla, M.; Rao, B. D.; Sreedevi, S.; Ruysschaert, J.-M.; Covey, D. F.; Chattopadhyay, A. Stereospecific requirement of cholesterol in the function of the serotonin$_{1A}$ receptor. *Biochim. Biophys. Acta, Biomembr.* **2014**, *1838*, 158−163.

(37) Krishnamoorthy, G.; Ira. Fluorescence lifetime distribution in characterizing membrane heterogeneity. *J. Fluoresc.* **2001**, *11*, 247−253.
(38) Mukherjee, S.; Kombrabail, M.; Krishnamoorthy, G.; Chattopadhyay, A. Dynamics and heterogeneity of bovine hippocampal membranes: role of cholesterol and proteins. *Biochim. Biophys. Acta, Biomembr.* **2007**, *1768*, 2130−2144.
(39) Mukherjee, S.; Raghuraman, H.; Chattopadhyay, A. Membrane localization and dynamics of Nile Red: effect of cholesterol. *Biochim. Biophys. Acta, Biomembr.* **2007**, *1768*, 59−66.
(40) Haugland, R. P. *Handbook of Fluorescent Probes and Research Chemicals*, 6th ed.; Molecular Probes Inc.: Eugene, OR, U.S.A., 1996.
(41) Shrivastava, S.; Paila, Y. D.; Dutta, A.; Chattopadhyay, A. Differential effects of cholesterol and its immediate biosynthetic precursors on membrane organization. *Biochemistry* **2008**, *47*, 5668−5677.
(42) Brochon, J.-C. Maximum entropy method of data analysis in time-resolved spectroscopy. *Methods Enzymol.* **1994**, *240*, 262−311.
(43) Swaminathan, R.; Krishnamoorthy, G.; Periasamy, N. Similarity of fluorescence lifetime distributions for single tryptophan proteins in the random coil state. *Biophys. J.* **1994**, *67*, 2013−2023.
(44) Swaminathan, R.; Periasamy, N. Analysis of fluorescence decay by the maximum entropy method: influence of noise and analysis parameters on the width of the distribution of lifetimes. *Proc. Indian Acad. Sci. (Chem. Sci.)* **1996**, *108*, 39.
(45) Greenspan, P.; Fowler, S. D. Spectrofluorometric studies of the lipid probe, Nile Red. *J. Lipid Res.* **1985**, *26*, 781−789.
(46) Dutta, A. K.; Kamada, K.; Ohta, K. Spectroscopic studies of Nile Red in organic solvents and polymers. *J. Photochem. Photobiol., A* **1996**, *93*, 57−64.
(47) Ghoneim, N. Photophysics of Nile Red in solution: steady state spectroscopy. *Spectrochim. Acta, Part A* **2000**, *56*, 1003−1010.
(48) Ira; Krishnamoorthy, G. Probing the link between proton transport and water content in lipid membranes. *J. Phys. Chem. B* **2001**, *105*, 1484−1488.
(49) Thewalt, J. L.; Bloom, M. Phosphatidylcholine: cholesterol phase diagrams. *Biophys. J.* **1992**, *63*, 1176−1181.
(50) Mouritsen, O. G. The liquid-ordered state comes of age. *Biochim. Biophys. Acta, Biomembr.* **2010**, *1798*, 1286−1288.
(51) Krishna, M. M. G.; Periasamy, N. Fluorescence of organic dyes in lipid membranes: Site of solubilization and effects of viscosity and refractive index on lifetimes. *J. Fluoresc.* **1998**, *8*, 81−91.
(52) Balcom, B. J.; Petersen, N. O. Lateral diffusion in model membranes is independent of the size of the hydrophobic region of molecules. *Biophys. J.* **1993**, *65*, 630−637.
(53) Wu, E.-S.; Jacobson, K.; Papahadjopoulos, D. Lateral diffusion in phospholipid multibilayers measured by fluorescence recovery after photobleaching. *Biochemistry* **1977**, *16*, 3936−3941.
(54) Derzko, Z.; Jacobson, K. Comparative lateral diffusion of fluorescent lipid analogues in phospholipid multibilayers. *Biochemistry* **1980**, *19*, 6050−6057.
(55) Schneider, M. B.; Chan, W. K.; Webb, W. W. Fast diffusion along defects and corrugations in phospholipid $P_{\beta'}$ liquid crystals. *Biophys. J.* **1983**, *43*, 157−165.
(56) Bultmann, T.; Vaz, W. L. C.; Melo, E. C. C.; Sisk, R. B.; Thompson, T. E. Fluid-phase connectivity and translational diffusion in a eutectic, two-component, two-phase phosphatidylcholine bilayer. *Biochemistry* **1991**, *30*, 5573−5579.
(57) Crane, J. M.; Tamm, L. K. Role of cholesterol in the formation and nature of lipid rafts in planar and spherical model membranes. *Biophys. J.* **2004**, *86*, 2965−2979.
(58) Pucadyil, T. J.; Mukherjee, S.; Chattopadhyay, A. Organization and dynamics of NBD-labeled lipids in membranes analyzed by fluorescence recovery after photobleaching. *J. Phys. Chem. B* **2007**, *111*, 1975−1983.
(59) Sankaram, M. B.; Thompson, T. E. Cholesterol-induced fluid-phase immiscibility in membranes. *Proc. Natl. Acad. Sci. U. S. A.* **1991**, *88*, 8686−8690.
(60) Brown, D. A.; London, E. Structure and origin of ordered lipid domains in biological membranes. *J. Membr. Biol.* **1998**, *164*, 103−114.
(61) Sinha, M.; Mishra, S.; Joshi, P. G. Liquid-ordered microdomains in lipid rafts and plasma membrane of U-87 MG cells: a time-resolved fluorescence study. *Eur. Biophys. J.* **2003**, *32*, 381−391.
(62) Haldar, S.; Kombrabail, M.; Krishnamoorthy, G.; Chattopadhyay, A. Depth-dependent heterogeneity in membranes by fluorescence lifetime distribution analysis. *J. Phys. Chem. Lett.* **2012**, *3*, 2676−2681.
(63) Chakraborty, H.; Haldar, S.; Chong, P. L.-G.; Kombrabail, M.; Krishnamoorthy, G.; Chattopadhyay, A. Depth-dependent organization and dynamics of archaeal and eukaryotic membranes: Development of membrane anisotropy gradient with natural evolution. *Langmuir* **2015**, *31*, 11591−11597.
(64) Chakraborty, H.; Lentz, B. R.; Kombrabail, M.; Krishnamoorthy, G.; Chattopadhyay, A. Depth-dependent membrane ordering by hemagglutinin fusion peptide promotes fusion. *J. Phys. Chem. B* **2017**, *121*, 1640−1648.
(65) Chattopadhyay, A.; London, E. Parallax method for direct measurement of membrane penetration depth utilizing fluorescence quenching by spin-labeled phospholipids. *Biochemistry* **1987**, *26*, 39−45.
(66) Haldar, S.; Chaudhuri, A.; Chattopadhyay, A. Organization and dynamics of membrane probes and proteins utilizing the red edge excitation shift. *J. Phys. Chem. B* **2011**, *115*, 5693−5706.
(67) Chattopadhyay, A.; Haldar, S. Dynamic insight into protein structure utilizing red edge excitation shift. *Acc. Chem. Res.* **2014**, *47*, 12−19.
(68) Haldar, S.; Kanaparthi, R. K.; Samanta, A.; Chattopadhyay, A. Differential effect of cholesterol and its biosynthetic precursors on membrane dipole potential. *Biophys. J.* **2012**, *102*, 1561−1569.
(69) Clarke, R. J. The dipole potential of phospholipid membranes and methods for its detection. *Adv. Colloid Interface Sci.* **2001**, *89*−*90*, 263−281.
(70) Singh, P.; Haldar, S.; Chattopadhyay, A. Differential effect of sterols on dipole potential in hippocampal membranes: implications for receptor function. *Biochim. Biophys. Acta, Biomembr.* **2013**, *1828*, 917−923.
(71) Bandari, S.; Chakraborty, H.; Covey, D. F.; Chattopadhyay, A. Membrane dipole potential is sensitive to cholesterol stereospecificity: implications for receptor function. *Chem. Phys. Lipids* **2014**, *184*, 25−29.
(72) Sarkar, P.; Chakraborty, H.; Chattopadhyay, A. Differential membrane dipolar orientation induced by acute and chronic cholesterol depletion. *Sci. Rep.* **2017**, *7*, 4484.
(73) Starke-Peterkovic, T.; Turner, N.; Vitha, M. F.; Waller, M. P.; Hibbs, D. E.; Clarke, R. J. Cholesterol effect on the dipole potential of lipid membranes. *Biophys. J.* **2006**, *90*, 4060−4070.
(74) Paila, Y. D.; Chattopadhyay, A. Membrane cholesterol in the function and organization of G-protein coupled receptors. *Subcell. Biochem.* **2010**, *51*, 439−466.
(75) Jafurulla, M.; Chattopadhyay, A. Membrane lipids in the function of serotonin and adrenergic receptors. *Curr. Med. Chem.* **2012**, *20*, 47−55.

https://dx.doi.org/10.1021/acs.jpcb.0c04338
J. Phys. Chem. B 2020, 124, 6312−6320